Ni/Pd core/shell nanoparticles supported on graphene as a highly active and reusable catalyst for Suzuki–Miyaura cross-coupling reaction

Önder Metin[1,2] (✉), Sally Fae Ho[1], Cemalettin Alp[2,4], Hasan Can[2], Max N. Mankin[1], Mehmet Serdar Gültekin[2], Miaofang Chi[3], and Shouheng Sun[1] (✉)

[1] *Department of Chemistry, Brown University, Providence, Rhode Island 02912, USA*

[2] *Department of Chemistry, Faculty of Science, Atatürk University 25240, Erzurum, Turkey*

[3] *Materials Science and Technology Division, Oak Ridge National Laboratory, Oak Ridge, Tennessee 37831, USA*

[4] *Çayırlı Vocational School, Erzincan University, Erzincan, Turkey*

ABSTRACT

Monodisperse Ni/Pd core/shell nanoparticles (NPs) have been synthesized by sequential reduction of nickel(II) acetate and palladium(II) bromide in oleylamine (OAm) and trioctylphosphine (TOP). The Ni/Pd NPs have a narrow size distribution with a mean particle size of 10 nm and a standard deviation of 5% with respect to the particle diameter. Mechanistic studies showed that the presence of TOP was essential to control the reductive decomposition of Ni–TOP and Pd–TOP, and the formation of Ni/Pd core/shell NPs. Using the current synthetic protocol, the composition of the Ni/Pd within the core/shell structure can be readily tuned by simply controlling the initial molar ratio of the Ni and Pd salts. The as-synthesized Ni/Pd core/shell NPs were supported on graphene (G) and used as catalyst in Suzuki–Miyaura cross-coupling reactions. Among three different kinds of Ni/Pd NPs tested, the Ni/Pd (Ni/Pd = 3/2) NPs were found to be the most active catalyst for the Suzuki–Miyaura cross-coupling of arylboronic acids with aryl iodides, bromides and even chlorides in a dimethylformamide/water mixture by using K_2CO_3 as a base at 110 °C. The G–Ni/Pd was also stable and reusable, providing 98% conversion after the 5th catalytic run without showing any noticeable Ni/Pd composition change. The G–Ni/Pd structure reported in this paper combines both the efficiency of a homogeneous catalyst and the durability of a heterogeneous catalyst, and is promising catalyst candidate for various Pd-based catalytic applications.

1   Introduction

Palladium (Pd) is one of the most popular metals used to catalyze chemical reactions such as carbon–carbon coupling [1], alcohol oxidation [2], olefin hydrogenation [3] and electrochemical formic acid oxidation [4]. Pd nanoparticles (NPs), due to their high surface-to-volume ratio, have been tested extensively as robust catalysts

for reaction kinetics tuning and optimization [5, 6]. However, catalytic reactions occur only on the surface of a Pd NP catalyst and a large fraction of Pd atoms in the core are catalytically inactive [7]. For instance, according to the full-shell "magic number" clusters model, a 5 nm close-packed metal NP has only 35% of total atoms exposed to an external reaction medium [8]. To make a large percentage of Pd atoms available for catalysis and to reduce Pd usage without sacrificing the overall catalytic performance, the core/shell NP concept has been introduced [9]. In this core/shell structure, the inner Pd is replaced by other non-noble metals and the presence of a different metal core provides some key controls over catalytic activity, selectivity and stability owing to "synergistic effects" arising from core–shell metal interaction and Pd shell lattice distortion [10]. Initial efforts in producing bimetallic Pd-based core/shell NPs led to the formation of Pd/Ni NPs that were not suitable for studying Pd catalysis because Pd is embedded under a Ni shell [11]. Catalytically active core/shell NPs were synthesized either by deposition of Pd on the preformed Ni NPs to form 5–7 nm Ni/Pd NPs for CO oxidation [12], or by consecutive thermal decomposition of Pd– and Ni–trioctylphosphine (TOP) complexes in oleylamine (OAm) to form Ni-rich core/Pd-rich shell NPs for the Sonogashira coupling reaction [13]. Additionally, Li et al. reported the one-pot synthesis of Pd–Ni alloy NPs and their catalysis of the Suzuki–Miyaura coupling reaction [14]. Recently, we synthesized monodisperse CoPd and CuPd NPs using OAm as both solvent and surfactant in the presence of a trace amount of TOP [15, 16]. We found that this approach could also be extended to prepare monodisperse Ni/Pd NPs that served as an excellent core/shell model for studying Pd catalysis.

Here we report the synthesis of monodisperse Ni/Pd NPs for the Suzuki–Miyaura cross-coupling reaction. The Suzuki–Miyaura cross-coupling reaction of aryl halides with arylboronic acids has emerged as one of the most powerful, attractive and convenient synthetic routes for the construction of biaryls that are important compounds in medicinal chemistry [17, 18]. Pd, especially a homogeneous Pd complex, is inevitably the catalyst choice for these coupling reactions due to the short reaction time and high synthetic yield/selectivity [19]. However, the recovery of homogeneous Pd complexes from the reaction mixture is difficult and the catalyst cannot be readily recycled for the next round of reaction. The problem may be solved by using supported Pd-based NPs as a catalyst [20, 21]. In this study, the Ni/Pd catalyst is prepared by supporting the Ni/Pd core/shell NPs on graphene (G) that has a large surface area and excellent chemical stability [22]. The G–Ni/Pd is highly active for Suzuki–Miyaura coupling of arylboronic acids with aryl iodides, bromides and even chlorides in a dimethylformamide/water mixture by using K_2CO_3 as a base at 110 °C. The catalyst is also stable and reusable, providing 98% conversion after the 5th run without showing any noticeable Ni/Pd composition change. The G–Ni/Pd NPs are a new class of catalyst for efficient Suzuki–Miyaura coupling reactions.

2   Experimental

2.1   Materials

Palladium(II) bromide (99%), oleylamine (technical grade, 70%), trioctylphosphine (90%), hexane (98.5%), isopropanol (99.5%), ethanol (100%), activated carbon (DARCO®-100 mesh particle size), aluminum oxide nanopowder (< 50 nm (BET)) and all reagents for Suzuki–Miyaura coupling reactions were purchased from Sigma–Aldrich and used as received. Nickel(II) acetate tetrahydrate (98%) was purchased from Strem Chemicals.

2.2   Characterization

Samples for transmission electron microscopy (TEM) analysis were prepared by depositing a single drop of diluted NP dispersion in hexane on amorphous carbon coated copper grids. Images were obtained using a JEOL 2010 TEM (200 kV). X-ray diffraction (XRD) patterns of the samples were collected on a Bruker AXS D8-Advance diffractometer with Cu-Kα radiation (λ = 1.5418 Å). Inductively coupled plasma–atomic emission spectroscopy (ICP–AES) measurements were carried out on a JY2000 Ultrace ICP Atomic Emission Spectrometer equipped with a JY AS 421 auto sampler and 2,400 g/mm holographic grating.

2.3   Synthesis of monodisperse Ni/Pd core/shell NPs

49.7 mg of nickel(II) acetate tetrahydrate (Ni(ac)$_2$·4H$_2$O, 0.2 mmol) and 53.4 mg of palladium(II) bromide (PdBr$_2$, 0.2 mmol) were mixed with 18.0 mL of OAm and 0.3 mL of TOP at room temperature. The reaction was heated to 245 °C at a rate of 5 °C/min under a gentle argon flow. A gradual color change from yellow-green to dark brown was observed during the synthesis indicating the nucleation and subsequent particle growth. The reaction mixture was then kept at 245 °C for 1 h before being cooled down to room temperature. The NP product was separated from the reaction mixture by adding isopropanol (40 mL), followed by centrifugation (8,500 rpm, 8 min). The NPs were further purified and collected by dispersing them into hexane (5 mL), adding an equivalent mixture of ethanol and isopropanol, and centrifuging at 8,500 rpm for 8 min. The product was redispersed in hexane. The synthesis yielded Ni/Pd core/shell NPs with Ni/Pd = 3/2. Under the same reaction conditions, 62.2 mg of Ni(ac)$_2$·4H$_2$O (0.25 mmol) and 53.4 mg of PdBr$_2$ (0.2 mmol) gave Ni/Pd (Ni/Pd = 7/3) and 49.7 mg of Ni(ac)$_2$·4H$_2$O (0.2 mmol) and 80 mg of PdBr$_2$ (0.3 mmol) led to the formation of Ni/Pd (Ni/Pd = 2/3).

2.4   Graphene synthesis

A single sheet of graphene oxide (GO) was synthesized from natural graphite powder by exfoliation of GO under ultrasonication in dimethylformamide (DMF) [23]. The DMF dispersion of GO (0.5 mg/mL) was heated to reflux for 6 h and the solution was then cooled down to room temperature to convert GO to G [24].

2.5   Supporting the Ni/Pd core/shell NPs on G and other supports

In a typical procedure, 10 mg of the Ni/Pd core/shell NPs were dissolved in 5.0 mL of hexane and mixed with 30.0 mg of G in DMF. The DMF/hexane mixture was sonicated for 2 h to ensure complete adsorption of NPs onto G. Then, the resultant mixture was centrifuged at 8,000 rpm for 10 min and the separated catalyst was washed twice with ethanol. The Ni/Pd core/shell NPs were also supported on activated carbon and aluminum oxide nanopowder by using same method and catalyst loading described above.

2.6   General procedure for G–Ni/Pd catalyzed Suzuki–Miyaura cross-coupling reactions

Suzuki–Miyaura cross-coupling reactions were conducted as follows: A mixture of aryl halides (2.0 mmol), phenylboronic acid (0.82 mmol) or 3-chloro-4-fluorophenylboronic acid (0.82 mmol), base (1.64 mmol), G–Ni/Pd catalyst (10 mg, 20 wt.% NPs and 0.0075 mmol Pd) and 10.0 mL of solvent mixture of DMF and water (v/v = 7/3) were mixed in a Schlenk tube (25 mL) and the mixture was vigorously stirred at 110 °C under air atmosphere. The progress of the reaction was monitored by thin layer chromatography (TLC). Upon reaction completion, the mixture was cooled to room temperature and the products were extracted with ethyl acetate (2 × 25 mL). The ethyl acetate phase was dried over sodium sulphate and evaporated at 55 °C under 8 mbar vacuum, filtered through a pad of silica gel with copious washing, concentrated and purified by flash chromatography on silica gel. The purity of the compounds was first evaluated by ^{1}H nuclear magnetic resonance (NMR) spectroscopy and then gas chromatography (GC). The yields were calculated from the ^{1}H-NMR spectra based on aryl halides.

2.7   Reusability of G–Ni/Pd catalyst in Suzuki–Miyaura cross-coupling reactions

The reusability test of the G–Ni/Pd (Ni/Pd = 3/2) catalyst (10 mg, 20 wt.% NPs and 0.0075 mmol Pd) in the Suzuki–Miyaura cross-coupling reaction between phenyl iodide (2.0 mmol) and phenylboronic acid (0.82 mmol) was performed five times as described in the section "*General procedure for Suzuki–Miyaura cross-coupling reactions*". After the first catalytic run, the G–Ni/Pd catalyst was separated from reaction solution by centrifugation (10,000 rpm, 10 min) and was reused in the next catalytic run.

3   Results and discussion

3.1   Synthesis of monodisperse Ni/Pd NPs

Monodisperse Ni/Pd core/shell NPs were synthesized via a one-pot high temperature solution phase synthesis including the consecutive reduction of nickel (II)

acetate and palladium(II) bromide in OAm and TOP. In our synthesis protocol, OAm acted the solvent, reducing agent and surfactant, and TOP served as a co-surfactant. Figure 1(a) shows a representative TEM image of the as-synthesized Ni/Pd NP array obtained by self-assembly of NPs after hexane was evaporated from the NP dispersion at room temperature. The Ni/Pd NPs have a narrow size distribution with a mean particle size of 10 nm and a standard deviation of 5% with respect to the particle diameter and are in a hexagonal close-packing with interparticle spacing at ~5 nm due to the coating of OAm and TOP on the NP surface. A high-resolution TEM (HR-TEM) image of Ni/Pd NPs shows that each NP has a polycrystalline structure. Some of the lattice fringes have a distance of ~0.232 nm, which is close to the lattice spacing of the (111) planes of the face-centered cubic (fcc) Pd crystal (0.223 nm). However, some periodic lattice fringes have a spacing of 0.337 nm ± 0.013 nm, where the error corresponds to the standard deviation in the measurement. This spacing is too large for any expected lattice fringe distance projected along the [111], [200], and [220] directions for face-centered

cubic (fcc) Ni and/or Pd. We attribute these to Moiré fringes, which stem from interference due to the superimposition of two misfit crystalline lattices (Pd and Ni lattices) [25]. Assuming no significant rotation, the spacing of Moiré fringes, D, was calculated to be ~0.337 nm by using the following expression:

$$D = \frac{d_1 d_2}{d_1 - d_2}$$

where d_1 and d_2 are the misfit periodicities of the two crystalline lattices. If we further assume that there is no semi-epitaxial growth, then such a Moiré spacing corresponds closely to Pd (200) on a Ni (220) plane (0.344 nm). The slight disagreement may stem from imaging on the improper zone axis of the [200] and [220] directions, a slight error in calibration of the TEM, or a slight rotation of the Pd layer with respect to the Ni core, which was not accounted for in the simple analysis above. To further prove that the core/shell structure is indeed formed, a high-angle annular dark-field scanning tunneling electron microscopy (HAADF–STEM) image was taken and a high resolution elemental mapping was done on a single Ni/Pd NP, as shown in Figs. 1(c) and 1(d). We can see a clearly defined core/shell structure with Ni atoms centered in the core (red) (~7.4 nm) and Pd atoms (green) (~1.3 nm) surrounding around the Ni core.

Metal contents in the Ni/Pd core/shell NPs were analyzed by ICP-AES. Using the current synthetic protocol, we can readily tune the composition of the Ni/Pd within the core/shell structure by simply controlling the initial molar ratio of the Ni and Pd salts. For instance, Ni/Pd NPs with Ni/Pd = 2/3, 3/2, or 7/3 were obtained if metal salts with the Ni/Pd ratio of 2:3, 1:1, or 5:4 were present during the synthesis. TEM images (Fig. S1 in the Electronic Supplementary Material (ESM)) show that the change in Ni/Pd composition does not affect the Ni/Pd NP morphology.

In the current synthesis, the use of TOP was found to be essential in the formation of monodisperse Ni/Pd NPs, which further supports the earlier observation that TOP is important for Ni- and Pd-salt reduction and decomposition [13]. Without TOP, Ni/Pd NPs could not be prepared. Complexation of TOP with Ni and Pd provides the necessary consecutive reduction
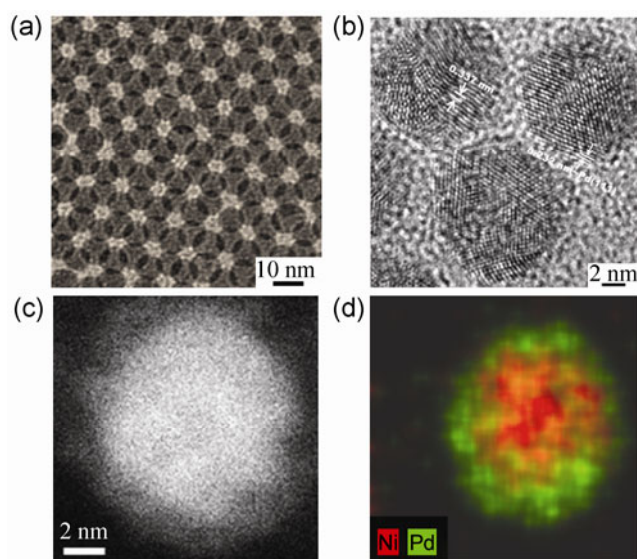
Figure 1 (a) TEM images of a 10 nm Ni/Pd NP array obtained from self-assembly of the NPs after hexane evaporation; (b) HR-TEM image and (d) XRD pattern of as synthesized Ni/Pd NPs; (c) the HAADF-STEM image of a 10 nm Ni/Pd (3/2) NP and (d) the corresponding high resolution elemental mapping of this 10 nm Ni/Pd NP. Red highlights the Ni and green denotes Pd distribution within Ni/Pd NP.

of Ni and Pd salts, leading to the formation of Ni/Pd NPs. Energy dispersive X-ray spectroscopy (EDS) shows a phosphorus peak, signifying the presence of the phosphine ligand on the surface of the NPs, whereas the nitrogen peak from the OAm is not detected (Fig. S2 (in the ESM)). Predominant phosphine coverage on the Ni/Pd NP is not unexpected as phosphorus is capable of forming π-back bonding with surface Pd, making a Pd–P bond stronger than a Pd–N coordination bond. The effect of TOP on the decomposition temperature of the metal precursors was studied. In the case of Ni, the Ni-TOP complex decomposed at 190 °C and this decomposition temperature was independent of the amount of TOP present in the reaction. However, the Pd–TOP complex decomposed above 200 °C and its decomposition temperature increased linearly as more TOP was added (Fig. 2). We can see that TOP does play an important role in controlling metal–TOP complex decomposition to form Ni/Pd NPs.

$$y = 14.346x + 191.55\ ℃$$
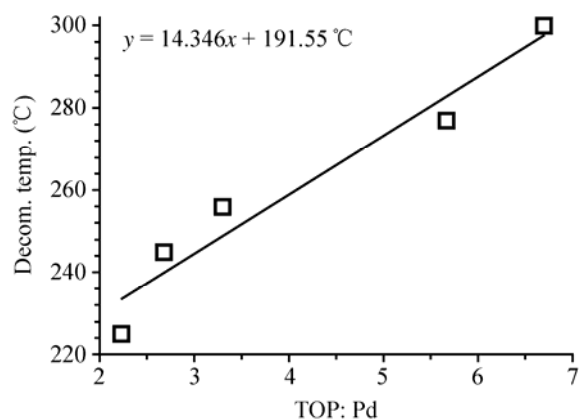
Figure 2 Decomposition temperature (decom. temp.) of the Pd–TOP complex as a function of the molar ratio of TOP:Pd.

Mechanistic studies were conducted to understand the process of NP formation by drawing out aliquots of the reaction at different time intervals and subsequently analyzing the samples via TEM (Fig. 3). NPs drawn 5 min after the reaction began were spherical in shape and appeared monodisperse. However, the shape of the NPs was distorted after 10 min and normalized after 30 min into the reaction. Because the Ni–TOP complex decomposes first, it is reasonable for Ni to nucleate and pre-form Ni NPs. As the reaction progresses, the Pd–TOP complex decomposes and Pd is able to nucleate and grow on the preformed Ni NPs. Therefore, we may attribute the morphology irregularity of the NPs at 10 min to the addition of Pd onto the Ni seeds. Given the difference in reduction potential between Pd and Ni (+0.915 V and –0.25 V (where we have used the standard reduction potential in water as an estimate)), it is also highly possible that some Ni serves as a sacrificial reducing agent for the Pd salt and initiates Pd nucleation on the Ni surface.

The effect of different phosphines on the formation of Ni/Pd NPs was also tested by replacing TOP with either tributylphosphine (TBP), triphenylphosphine (TPP), or tri-isopropylphosphine (TIP). The size of the NPs increased from 10 nm to ~15, 20, and 50 nm, respectively, along with a change in NP morphology change (Fig. S3 (in the ESM)). Considering the cone angles of TIP (160°), TPP (145°), TBP (130°), the ligand with the largest cone angle produces the largest NPs under our reaction conditions. The long octyl chains of the TOP are not only able to stabilize the NPs, but prevent excess precursor from adding to the existing NPs, thereby restricting the size to 10 nm. However, the shorter and bulkier phenyl, butyl and tri-isopropyl
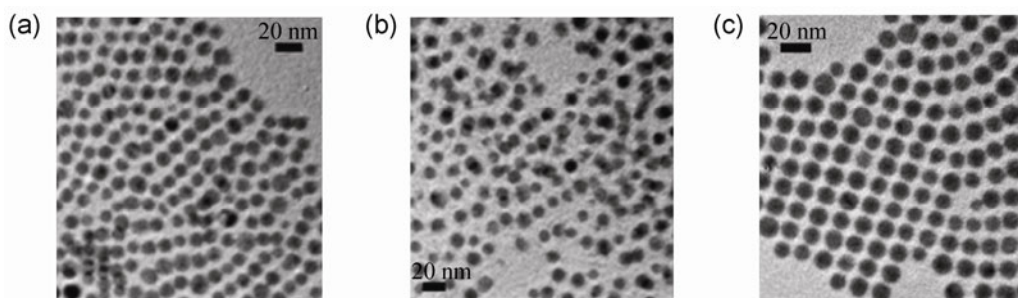
Figure 3 TEM images of NPs isolated from aliquots extracted from the synthesis of 10 nm Ni/Pd core/shell NPs at intervals after the start of the nucleation process: (a) 5 min, (b) 15 min, (c) 45 min.

ligands facilitate NP growth, resulting in larger NPs.

3.2 Suzuki–Miyaura cross-coupling reactions catalyzed by G–Ni/Pd catalyst

To use Ni/Pd NPs in the Suzuki–Miyaura cross-coupling reaction, we first deposited them on G via a liquid phase self-assembly method including the sonication of DMF dispersion of G and hexane dispersion of NPs [26]. Figure 4(a) shows a TEM image of the as-prepared G–Ni/Pd catalyst. The Ni/Pd NPs are well-dispersed on the G sheet and preserve their initial morphology and size. This G–Ni/Pd catalyst was then tested directly in the Suzuki–Miyaura cross-coupling reaction without any further surfactant removal treatment.

The G–Ni/Pd NPs were first tested as catalysts for the Suzuki–Miyaura cross-coupling reaction between phenyl iodide and phenylboronic acid by using different bases (NaOH, K_2CO_3, potassium t-butoxide (^tBuOK), triethylamine (NEt$_3$)) in dimethylformamide/ water (DMF:H_2O) mixtures [27]. The DMF/H_2O mixture was selected as the solvent due to the good dispersion of G in DMF and high solubility of arylboronic acids in water. We found that the Suzuki–Miyaura coupling reaction catalyzed by G–Ni/Pd gave the highest yield when DMF/H_2O (v/v = 7:3) was used as a solvent in the presence of K_2CO_3 as a base at 110 °C. Under this reaction condition, we also evaluated the catalysis of G–Ni/Pd NPs with different Ni/Pd ratios at 2/3, 3/2, and 7/3 in the coupling between phenyl iodide and phenylboronic acid. We found G–Ni/Pd (Ni/Pd = 3/2) to be the most active catalyst, giving 99% yield in 10 min. Therefore, we used this G–Ni/Pd catalyst to

study all other Suzuki–Miyaura couplings between aryl halides and phenylboronic acids.
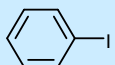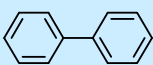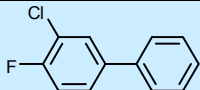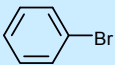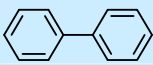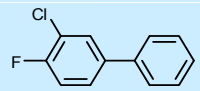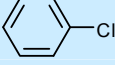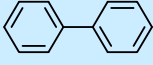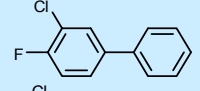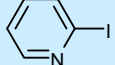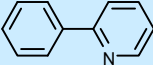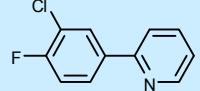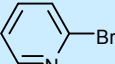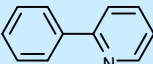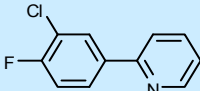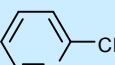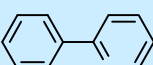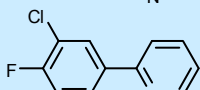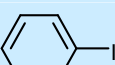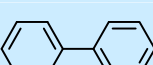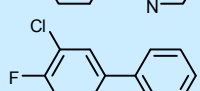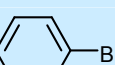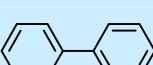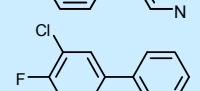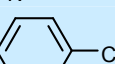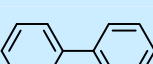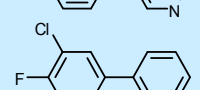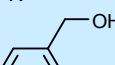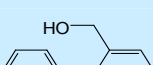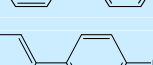
The G–Ni/Pd catalyzed Suzuki–Miyaura coupling reactions of different substrates are summarized in Table 1. We can see that the couplings between phenylboronic acid or 3-chloro-4-fluorophenylboronic acid and phenyl iodide or iodopyridine produce biaryls in excellent yields in 10 min (Table 1, entries 1, 4, 7, 10, and 11). The G–Ni/Pd catalyst is also efficient in the coupling between Br-substituted phenyls or pyridines with the yields reaching 80% in 30 min (Table 1, entries 2, 5, 8). The G–Ni/Pd catalyst works even well for aryl chlorides, that are often less reactive under the common Suzuki–Miyaura coupling reaction conditions (Table 1, entries 3, 6, 9, 12). Considering the low Pd content in the core/shell structure, the G–Ni/Pd catalyst shows much higher activity than most of the Pd NP catalyst systems previously tested in the Suzuki–Miyaura cross-coupling reaction [28]. We believe that the high activity of the G–Ni/Pd catalyst stems from the good dispersion of G in the DMF/water mixture (v/v = 7/3), and the presence of a graphitic plane near each G–Ni/Pd NP in G–Ni/Pd helps to adsorb the aromatic component in the reactant mixture, pulling them in close range contact with Ni/Pd for Pd catalysis. To prove this point, we evaluated the catalytic activity of Ni/Pd NPs on activated carbon (C–Ni/Pd) and aluminum oxide nanopowder (Al_2O_3–Ni/Pd) in the couplings between phenylboronic acid and phenyl bromide or phenyl chloride under the same reaction conditions and with same catalyst loading (Table S1 (in the ESM)). We can see that the C–Ni/Pd and Al_2O_3–Ni/Pd catalysts
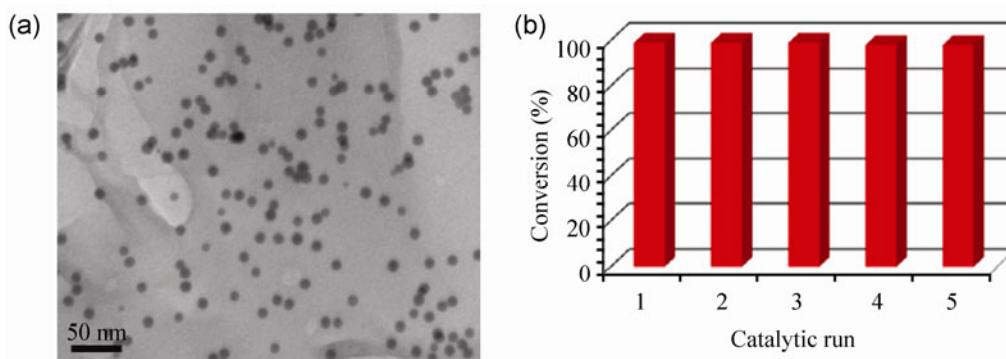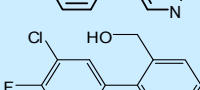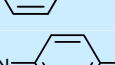

Figure 4 (a) TEM image of as-prepared G–Ni/Pd catalyst (20 wt.% NiPd loading); and (b) the five runs reusability test of G–Ni/Pd catalyst in the Suzuki–Miyaura coupling of phenyl iodide and phenylboronic acids under the optimized conditions.

Table 1 G–Ni/Pd (Ni/Pd = 3/2) catalyzed Suzuki–Miyaura cross-coupling reaction of various aryl halides and pyridine halides with phenylboronic acid or 3-chloro-4-fluorophenylboronic acid

$$Ar - X + Ar' - B(OH)_2 \xrightarrow[\text{G-Ni/Pd catalyst (10 mg)}]{K_2CO_3,\ DMF:H_2O(7:3,\ 10\,mL),\ 110\,^{\circ}C} Ar - Ar'$$

X: I, Br, Cl

Entry	Ar–X	Time	Yield (%)[a]	Product[a]	Yield (%)[b]	Product[b]
1	phenyl–I	10 min	99, 98[c]	biphenyl	98	3-chloro-4-fluoro-biphenyl
2	phenyl–Br	30 min	78	biphenyl	91	3-chloro-4-fluoro-biphenyl
3	phenyl–Cl	3h	45	biphenyl	65	3-chloro-4-fluoro-biphenyl
4	2-pyridyl–I	10 min	95	phenylpyridine	98	chloro-fluoro-phenylpyridine
5	2-pyridyl–Br	30 min	80	phenylpyridine	91	chloro-fluoro-phenylpyridine
6	2-pyridyl–Cl	3h	45	phenylpyridine	60	chloro-fluoro-phenylpyridine
7	3-pyridyl–I	10 min	99	phenylpyridine	99	chloro-fluoro-phenylpyridine
8	3-pyridyl–Br	30 min	83	phenylpyridine	95	chloro-fluoro-phenylpyridine
9	3-pyridyl–Cl	3h	50	phenylpyridine	70	chloro-fluoro-phenylpyridine
10	2-(hydroxymethyl)phenyl–I	10 min	95	HO-CH2-biphenyl	98	Cl,F-HO-CH2-biphenyl
11	O_2N-pyridyl-Cl	1h	92	phenyl-pyridine-NO_2	96	Cl,F-phenyl-pyridine-NO_2

Reaction conditions: 2.0 mmol of aryl halide, 0.82 mmol of phenylboronic acid or 3-chloro-4-fluorophenylboronic acid, 1.64 mmol K_2CO_3, 10.0 mL of DMF: water mixture (v/v = 7:3), 10.0 mg of G–Ni/Pd catalyst (20 wt.% NiPd, 0.0075 mmol Pd), 110 $^{\circ}$C; open air atmosphere. Purity of products was checked by ^{1}H-NMR and GC. [a] Coupling reaction with phenylboronic acid. [b] Coupling reaction with 3-chloro-4-fluorophenylboronic acid. [c] Yield after the 5th consecutive catalytic run.

afforded lower yields (65% and 45%, respectively) compared to G–Ni/Pd for the coupling between phenyl bromide and phenylboronic acid, but they are nearly inactive for the coupling of phenyl chloride and phenylboronic acid with only 10% and 5% yields.

Besides its high activity, the G–Ni/Pd catalyst is also stable and reusable for the Suzuki–Miyaura cross-coupling reaction, providing 98% conversion after its 5th consecutive use in the coupling reaction of phenyl iodide and phenylboronic acid (Fig. 4(b)). After the 5th run, the catalyst was further analyzed by TEM and ICP–AES. A TEM image of the G–Ni/Pd NPs revealed no change in NP morphology after the stability test (Fig. S4 (in the ESM)) and ICP–AES measurements showed that the Ni/Pd composition was preserved at the end of the reactions, indicating that there was no

leaching of either Ni or Pd from the G–Ni/Pd under the Suzuki–Miyaura coupling reaction conditions employed.

4   Conclusions

We have reported a one-pot synthesis of monodisperse 10 nm Ni/Pd core/shell NPs by sequential reduction of nickel(II) acetate and palladium(II) bromide in OAm and TOP. The core/shell structure of NPs was proved by a mechanistic study as well as advanced analytical techniques and the presence of TOP was found to be essential to control the reductive decomposition of Ni–TOP and Pd–TOP, and in the formation of Ni/Pd core/shell NPs. The composition of Ni/Pd NPs was controlled by the initial metal precursor ratios. The core/shell NPs were deposited on graphene (G) via a solution phase-based self-assembly method and the G–Ni/Pd NPs were tested to catalyze Suzuki–Miyaura coupling reactions. Among three different kinds of Ni/Pd NPs tested, the Ni/Pd (Ni/Pd = 3/2) NPs were found to be the most active catalyst for the coupling between various phenyl and pyridine halides and phenylboronic acid in DMF/water (v/v = 7/3) at 110 °C. The G–Ni/Pd catalyst was also stable and could be recycled for use in the cross-coupling reactions, providing 98% conversion after the 5th reaction run without noticeable leaching of Ni or Pd. The G–Ni/Pd structure reported here combines both the efficiency of a homogeneous catalyst and the durability of a heterogeneous catalyst, and is a promising catalyst candidate for various Pd-based catalytic applications.

Acknowledgements

Electronic Supplementary Material: Supplementary material (further characterization of Ni/Pd core/shell NPs and optimization experiments performed on Suzuki–Miyaura cross-coupling reactions) is available in online version of this article at http://dx.doi.org/ 10.1007/s12274-012-0276-4 and is accessible free of charge.

References

[1]   Barder, T. E.; Walker, S. D.; Martinelli, J. R.; Buchwald, S. L. Catalysts for Suzuki−Miyaura coupling processes Scope and studies of the effect of ligand structure. *J. Am. Chem. Soc.* **2005**, *127*, 4685–4696.

[2]   Kakiuchi, N.; Maeda, Y.; Nishumura, T.; Uemura, S. Pd(II)− hydrotalcite-catalyzed oxidation of alcohols to aldehydes and ketones using atmospheric pressure of air. *J. Org. Chem.* **2001**, *66*, 6620–6625.

[3]   Wang, Y. Q.; Lu, S. M.; Zhou, Y. G. Highly enantioselective Pd-catalyzed asymmetric hydrogenation of activated imines. *J. Org. Chem.* **2007**, *72*, 3729–3734.

[4]   Mazumder, V.; Sun, S. H. Oleylamine-mediated synthesis of Pd nanoparticles for catalytic formic acid oxidation. *J. Am. Chem. Soc.* **2009**, *131*, 4588–4589.

[5]   Reetz, M. T.; Westermann, E. Phosphane-free palladium-catalyzed coupling reactions: The decisive role of Pd nanoparticles. *Angew. Chem. Int. Ed.* **2000**, *39*, 165–168.

[6]   Kogan, V.; Aizenshtat, Z.; Popovitz-Biro, R.; Neumann, R. Carbon–carbon and carbon–nitrogen coupling reactions catalyzed by palladium nanoparticles derived from a palladium substituted Keggin-type polyoxometalate. *Org. Lett.* **2002**, *4*, 3529–3532.

[7]   Aiken, J. D.; Finke, R. G. A review of modern transition-metal nanoclusters: Their synthesis, characterization, and applications in catalysis. *J. Mol. Catal. A- Chem.* **1999**, *145*, 1–44.

[8]   Schmid, G. *Nanoparticles: From Theory to Application*; Wiley-VCH: Weinheim, 2004.

[9]   Ferrando, R.; Jellinek, J.; Johnston, R. L. Nanoalloys: From theory to applications of alloy clusters and nanoparticles. *Chem. Rev.* **2008**, *108*, 845–910.

[10]   Schmid, G.; Lehnert, A.; Malm, J. O.; Bovin, J. O. Ligand-stabilized bimetallic colloids identified by HRTEM and EDX. *Angew. Chem. Int. Ed.* **1991**, *30*, 874–876.

[11]   Teranishi, T.; Miyake, M. Novel synthesis of monodispersed Pd/Ni nanoparticles. *Chem. Mater.* **1999**, *11*, 3414–3416.

[12]   Sao-Joao, S.; Giorgio, S.; Penisson, J. M.; Chapon, C.; Bourgeois, S.; Henry, C. Structure and deformations of Pd–Ni core–shell nanoparticles. *J. Phys. Chem. B* **2005**, *109*, 342–347.

[13] Son, S. U.; Jang, Y.; Park, J.; Na, H. B.; Park, H. M.; Yun, H. J.; Lee, J.; Hyeon, T. Designed synthesis of atom-economical Pd/Ni bimetallic nanoparticle-based catalysts for Sonogashira coupling reactions. *J. Am. Chem. Soc.* **2004**, *126*, 5026–5027.

[14] Wu, Y. E.; Wang, D. S.; Zhao, P.; Niu, Z. Q.; Peng, Q.; Li, Y. D. Monodispersed Pd-Ni nanoparticles: Composition control synthesis and catalytic properties in the Miyaura–Suzuki reaction. *Inorg. Chem.* **2011**, *50*, 2046–2048.

[15] Sun, D. H.; Mazumder, V.; Metin, Ö.; Sun, S. H. Catalytic hydrolysis of ammonia borane via cobalt palladium nano-particles. *ACS Nano* **2011***, 5*, 6458–6464.

[16] Mazumder, V.; Chi, M. F.; Mankin, M. N.; Liu, Y.; Metin, Ö.; Sun, D. H.; More, K. L.; Sun, S. H. A facile synthesis of *M*Pd (*M* = Co, Cu) nanoparticles and their catalysis for formic acid oxidation. *Nano Lett.* **2012**, *12*, 1102–1106.

[17] Miyaura, N.; Yanagi, T.; Suzuki, A. The palladium-catalyzed cross-coupling reaction of phenylboronic acid with haloarenes in the presence of bases. *Synth. Commun.* **1981**, *11*, 513–519.

[18] Miyaura, N.; Suzuki, A. Palladium-catalyzed cross-coupling reactions of organoboron compounds. *Chem. Rev.* **1995**, *95,* 2457–2483.

[19] de Mejere, A.; Diederich, F. *Metal-Catalyzed Cross-Coupling Reactions*; Wiley-VCH: Weinheim, 2004.

[20] Astruc, D.; Lu, F.; Aranzaes, J. R. Nanoparticles as recyclable catalysts: The frontier between homogeneous and heterogeneous catalysis. *Angew. Chem. Int. Ed.* **2005**, *44*, 7852–7872.

[21] Metin, Ö.; Durap, F.; Aydemir, M.; Özkar, S. Palladium(0) nanoclusters stabilized by poly(4-styrenesulfonic acid-co-maleic acid) as an effective catalyst for Suzuki–Miyaura cross-coupling reactions in water. *J. Mol. Catal. A- Chem.* **2011**, *337*, 39–44.

[22] Metin, Ö.; Kayhan, E.; Özkar, S.; Schneider, J. J. Palladium nanoparticles supported on chemically derived graphene: An efficient and reusable catalyst for the dehydrogenation of ammonia borane. *Int. J. Hydrog. Energy* **2012**, *37*, 8161–8169.

[23] Guo, S. J.; Dong, S. J.; Wang, E. K. Three-dimensional Pt-on-Pd bimetallic nanodendrites supported on graphene nanosheet: Facile synthesis and used as an advanced nanoelectrocatalyst for methanol oxidation. *ACS Nano* **2010**, *4*, 547–555.

[24] Ai, K. L.; Liu, Y. L.; Lu, L. H.; Cheng, X. L.; Huo, L. H. A novel strategy for making soluble reduced graphene oxide sheets cheaply by adopting an endogenous reducing agent. *J. Mater. Chem.* **2011**, *21,* 3365–3370.

[25] Williams, D. B.; Carter, C. B. *Transmission Electron Microscopy: A Textbook for Materials Science*, *2nd Edition*; Kluwer Academic/Plenum: New York, 2009.

[26] Gao, S. J.; Sun, S. H. FePt nanoparticles assembled on graphene as enhanced catalyst for oxygen reduction reaction. *J. Am. Chem. Soc.* **2012**, *134*, 2492–2495.

[27] See supporting information for the optimization experiments performed on G-Ni/Pd catalyzed Suzuki–Miyaura cross-coupling reactions.

[28] For the catalytic activities of various Pd nanoparticles catalyst system tested in the Suzuki–Miyaura cross-couplings under similar conditions. See: Durap, F.; Metin, Ö.; Aydemir, M.; Özkar, S. New route to synthesis of PVP-stabilized palladium(0) nanoclusters and their enhanced catalytic activity in Heck and Suzuki cross-coupling reactions. *Appl. Organomet. Chem.* **2009**, *23*, 498–503.